Determining energy relaxation length scales in two-dimensional electron gases

Jordan Billiald, Dirk Backes, Jürgen König, Ian Farrer, David Ritchie, and Vijay Narayan

Determining energy relaxation length scales in two-dimensional electron gases

Jordan Billiald,[1] Dirk Backes,[1] Jürgen König,[2] Ian Farrer,[1] David Ritchie,[1] and Vijay Narayan[1]

[1]*Cavendish Laboratory, University of Cambridge, J. J. Thomson Avenue, Cambridge, CB3 0HE, United Kingdom*
[2]*Theoretische Physik and CENIDE, Universität Duisburg-Essen, 47048 Duisburg, Germany*

We present measurements of the energy relaxation length scale ℓ in two-dimensional electron gases (2DEGs). A temperature gradient is established in the 2DEG by means of a heating current, and then the elevated electron temperature T_e is estimated by measuring the resultant thermovoltage signal across a pair of deferentially biased bar-gates. We adapt a model by Rojek and König [Phys. Rev. B **90**, 115403 (2014)] to analyse the thermovoltage signal and as a result extract ℓ, T_e, and the power-law exponent α_i for inelastic scattering events in the 2DEG. We show that in high-mobility 2DEGs, ℓ can attain macroscopic values of several hundred microns, but decreases rapidly as the carrier density n is decreased. Our work demonstrates a versatile low-temperature thermometry scheme, and the results provide important insights into heat transport mechanisms in low-dimensional systems and nanostructures. These insights will be vital for practical design considerations of future nanoelectronic circuits. © 2015 AIP Publishing LLC.
[http://dx.doi.org/10.1063/1.4926338]

There currently exist well-established methods to probe the low-temperature (low-T) electrical and thermoelectric properties of two-dimensional electron gases (2DEGs). However, probing heat transport mechanisms in these systems has proven more challenging, primarily due to the lack of convenient low-T thermometers that couple directly to the electron gas. Conventional low-T thermometers such as germanium or ruthenium-oxide films are sensitive only to the lattice temperature T_L, the temperature of the crystal that hosts the 2DEG. At $T_L \lesssim 1\,K$, the coupling between electrons and phonons becomes relatively weak, and therefore T_e can differ significantly from T_L. The electrical resistance of the 2DEG itself becomes insensitive to T_e at these temperatures, since the majority of scattering events are from static impurities. These both therefore become ineffective at measuring T_e in this regime. Accurate measures of T_e can be obtained from the Coulomb-blockade characteristics of quantum dots[1] which are broadened at a finite T_e. The weak localization characteristics of 2DEGs[2] can also be useful as they depend sensitively on the phase-coherence length which is T_e-dependent. However, neither of these methods lends themselves easily to the measurement of spatial temperature gradients, which is required in order to measure the thermal conductivity κ (Refs. 3 and 4) or the energy relaxation length scale ℓ in 2DEGs.

Appleyard et al.[5] showed that the diffusive component of the thermopower S can be used to detect differences between T_e and T_L. Here, $S \equiv V_{th}/\Delta T$, where V_{th} is the thermovoltage developed in response to a temperature difference ΔT. To do this, they measured V_{th} across a pair of quantum point contacts (QPCs) with a heated electron gas between them, as was done similarly in Ref. 6, and more recently in Ref. 7. Then ΔT was estimated as V_{th}/S, where S was obtained using the Mott relation[8]

$$ S = \frac{\pi^2 k_B^2 T}{3e\hbar^2} \left(\frac{d \ln \sigma}{dE} \right)_{E=\mu}. \quad (1) $$

Here, k_B is the Boltzmann constant, e is the electron charge, $\hbar \equiv h/2\pi$ with h being Planck's constant, σ is the electrical conductivity, E is the total energy, and μ is the chemical potential. This technique has been used to measure κ in quantum wires[3,9] and energy-loss rates in 2DEGs.[10] Chickering et al.[11] showed Eq. (1) to be broadly valid in gated regions of a 2DEG between 0.8 K and 2 K and therein suggested the possibility of using a symmetric pair of bar-gates as a low-T thermometer for the electron gas. This method was recently employed to measure S in mesoscopic 2DEGs.[12–14] Usefully, the relatively large size of the bar-gates eliminates the need for electron beam lithography which simplifies the fabrication process. However, it was noted in Ref. 11 that the data systematically deviated from the Mott prediction. Rojek and König[15] attributed these deviations to the spatial extent of the bar-gate thermometers (BGTs) being comparable to the energy relaxation length ℓ in the 2DEG and developed a model to account for this. In this work, we adapt the model developed by Rojek and König to refine the analysis of the signal produced by a BGT, and to make an accurate measurement of ℓ.

Figure 1(a) shows a false-colour SEM image of a typical device. Please see the supplementary material[18] for wafer and fabrication details. The device consists of a heating element and a longitudinal strip of 2DEG (of width 100 μm and length $L_{strip} = 1\,mm$) which together form a 'T' shape, with three BGTs along the strip. The first BGT is at a distance $L_{T1} = 200\,\mu m$ from the heating element. A top-gate sits over the heating element and the strip and is used to tune the electron density n in these regions. This design minimizes any power reflection at the interface between the heating element

(a)

(b)
$$T_e = \Delta T + T_L$$

$$L_g \qquad L_{ug}$$

$$I \quad II \qquad III \quad IV$$
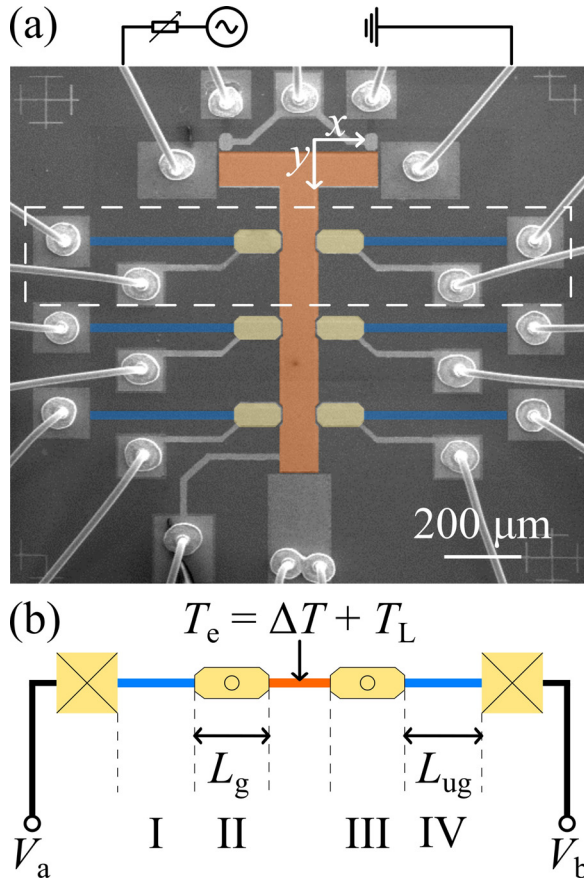
$$V_a \qquad\qquad\qquad V_b$$

FIG. 1. Device geometry. (a) False-colour SEM image of the device used in our experiments. The first bar-gate thermometer (BGT) is outlined by white dashed lines. The three contacts at the top of the device allow a four-terminal measurement of the heating element resistance. (b) Schematic representation of a BGT which consists of gated (II and III, yellow) and ungated (I and IV, blue) regions of 2DEG, terminated by an ohmic contact. The orange section between the gates illustrates a region of "hot" electrons.
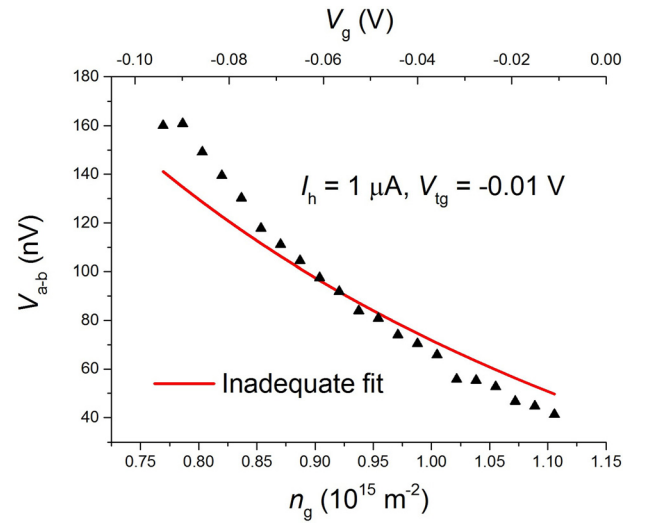

FIG. 2. The fit shown in this figure is based on a simple model where the hot electrons are assumed to relax to T_L within the gated region. This model ignores any effects of the temperature profile along the BGT, and therefore the only fitting parameter is T_e. The fit is clearly inadequate with the fit systematically deviating from the experimental data. This kind of deviation was found to be typical across the parameter space of I_h and V_{tg} explored in this experiment.

and the strip. The strip is terminated by a large ohmic contact.

Throughout the experiment all ohmic contacts through which no current is passed were assumed to be at T_L, since they are in direct thermal contact to the mixing chamber via the measurement wiring. Figure 1(b) shows a schematic of a single BGT. It is a symmetric structure consisting of two arms flanking the 2DEG strip. The left (right) arm is formed by a gated region labelled II (III), followed by an ungated region labelled I (IV), and terminated by an ohmic contact. The lengths of the gated and ungated regions of the arms are $L_g = 150\,\mu m$ and $L_{ug} = 455\,\mu m$, respectively.

The experiment involves passing a current I_h at frequency $f = 10\,Hz$ through the heating element which Joule heats the electron gas with a power of $I_h^2 R_h$, where R_h is the four-terminal electrical resistance of the heating element. This establishes a temperature gradient along the length of the 2DEG strip. The thermovoltage V_{th} generated across a thermometer in response to I_h is detected at $2f$ using a lock-in amplifier. Figure 2 shows $V_{th} = V_a - V_b$ (see Fig. 1(b)) from the first BGT while the gate voltage (V_g) on gate II is swept. An almost identical result is obtained when gate III is swept, except that V_{th} is opposite in sign. The thermovoltages developed across the second and third BGTs were found to be

negligible for even the largest used heating currents. Each section of the BGT from I to IV contributes to V_{th}

$$V_{th} = \sum_p S_p \Delta T_p. \qquad (2)$$

Here, p goes from I to IV, denoting each section shown in Fig. 1(b), ΔT_p is the temperature drop across section p, and S_p for each section is given by the Mott formula for a non-interacting 2DEG

$$S_p = \frac{\pi k_B^2 T_p m}{3e\hbar^2} \frac{(1 + \alpha_e)}{n_p}. \qquad (3)$$

Equation (3) is obtained by substituting the Drude expression $\sigma = n_p e^2 \tau_e / m$ for the electrical conductivity into Eq. (1). Here, n_p is the 2D number density of charge carriers in section p, τ_e is the Drude elastic scattering time, m is the effective mass of the charge carriers ($=0.067 m_e$ in GaAs-based 2DEGs, with m_e being the bare electron mass), $\alpha_e \equiv (n_p/\tau_e)(d\tau_e/dn_p)$, and T_p is the average electron temperature in region p.

Figure 2 also shows the best fit to the data by assuming that hot electrons relax to T_L within a distance L_g and therefore over the gated region, regardless of the carrier density n_g beneath the gate. In this simple picture, the temperature profile along the BGT arm is not relevant, and the only unknown is T_e between the BGT arms. However, the quality of the fit is clearly inadequate and this is found to be the case across the parameter space of I_h and V_{tg} explored in this experiment.

We first describe why it is essential to consider the contribution from *all* the regions $p = I$ to IV towards V_{th}. At low-T and especially in high-mobility 2DEGs, the energy relaxation length ℓ over which hot electrons relax through inelastic processes can greatly exceed the mean-free path of electrons.[15,17] The dependence of ℓ on the inelastic scattering time τ_i is given by $\ell \equiv \sqrt{D\tau_i}$, where $D = v_F^2 \tau_e/2$ is the

diffusion constant of the electrons, and v_F is the Fermi velocity. τ_i has a power-law dependence on n: $\tau_i = \tau_{i,0}(n/n_0)^{\alpha_i}$, where the subscript 0 denotes the values in the ungated 2DEG. Thus, the distance over which electrons lose their excess energy in the BGT arm is crucially dependent on n_p. The ohmic contact enforces $T_e = T_L$ at the 2DEG to ohmic contact interface, and this needs to be taken into consideration if ℓ is comparable to $L_g + L_{ug}$. Therefore, in all the above situations, both the gated and ungated regions contribute to V_{th} in a manner dependent on T_e at the centre of the BGT, T_e at the interface of the gated and ungated regions, ℓ, and α_i, all of which need to be estimated self-consistently. To do this we adapt the model used in Ref. 15 (described in the supplementary material[18]). The resulting expression for $\Delta T_e \equiv T_e - T_L$ at the junction of the gated and ungated regions $\Delta T_e(L_g)$ reads

$$\Delta T_e(L_g) = \Delta T_e \frac{z \sinh\left(L_{ug}/\ell_0\right)}{\cosh\left(L_{ug}/\ell_0\right)\sinh\left(L_g/\ell\right) + z \sinh\left(L_{ug}/\ell_0\right)\cosh\left(L_g/\ell\right)}. \tag{4}$$

Here, ℓ_0 is the energy relaxation length at $n = n_0$ and $z \equiv (n/n_0)^{(1+\alpha_e-\alpha_i)/2}$. Within the framework of the linearized model of Rojek *et al.*,[15] $T_p = T_L$. Equation (4) provides an expression for ΔT_p, which when substituted together with Eq. (3) in Eq. (2), results in an expression for V_{th} as a function of n_0, n in each gated region, ℓ_0, α_e, α_i, and T_e. We measure n_0 and $n(V_g)$ in the device by observing V_g-dependent edge-state reflections in the quantum Hall regime,[16] and α_e is extracted from the dependence of σ on n and turns out to be ≈ 0.89 over the relevant range of n. This leaves three unknowns, namely, ℓ_0, T_e, and α_i, which are used as fitting parameters. Importantly though, by fitting to several complementary datasets whilst varying different experimental parameters such as I_h and V_{tg}, we are able to considerably reduce the uncertainty in these three fitting parameters (see supplementary material[18]).

Figure 3(a) shows V_{th} against n_g for varying I_h which will produce different ΔT_e. Figure 3(b) shows V_{th} against n_g but for varying V_{tg} which will vary ℓ in the 2DEG strip as well as ΔT_e via its effect on R_h. Clearly, the model produces excellent fits to the data with no discernible systematic deviations. Similar data and quality of fit are obtained when the adjacent BGT is swept.

The results of the fitting are the ΔT_e for each I_h and V_{tg} in the two datasets. Figure 4(a) shows ΔT_e as a function of I_h on a log-log scale, and we find that $\Delta T_e \propto I_h^{1.65}$. This sub-squared dependence is presumably due to a fraction of the power being lost to the lattice and to the ohmic contacts. The values of α_i and ℓ_0 are found to be ≈ 3.76 and $\approx 280\,\mu\text{m}$, respectively. Figure 4(b) shows ΔT_e as a function of V_{tg} after

ΔT_e has been scaled for the changing value of R_h. This has been done by applying a corrective factor of $R_{h,0}/R_h(V_{tg})$, so that any change in ΔT_e is now due solely to a change in ℓ. Here, $R_h(V_{tg})$ is the electrical resistance of the heating element as a function of V_{tg}. Therefore, the graph suggests that for $V_{tg} \lesssim -0.11$ V, the hot electrons completely relax within a distance L_{T1}.

The data therefore suggest that hot electrons thermalize over macroscopic length scales ($\approx 300\,\mu\text{m}$) in the ungated 2DEG, but that this length scale rapidly decreases with n. This strongly justifies the need to account for the ungated 2DEG arms when using BGTs at high n_g. This is also consistent with the negligible thermovoltage detected across the second and third BGTs which are at distances of $500\,\mu\text{m}$ and $800\,\mu\text{m}$ from the heating element, respectively. While n_g can certainly be lowered until $\ell < L_g$, such that $\Delta T_e(L_g) = 0$, care must be taken to ensure that Eq. (3) remains valid. Indeed, we have observed that when the 2DEG approaches the localized regime (when σ becomes $\lesssim 3e^2/h$) the model is unable to fit the data satisfactorily. In this experiment, n was conservatively limited to $\geq 0.7 \times 10^{15}\,\text{m}^{-2}$ corresponding to $k_F l \geq 4$ and $r_s \leq 2$, where k_F is the Fermi wave vector, l is the elastic mean free path, and r_s is the interaction parameter defined as the ratio of the Coulomb energy and kinetic energy of the 2DEG.

Importantly, the model *only* provides the value of ℓ_0 and α_i from which $\ell(n)$ can be reconstructed. However, as argued in the previous paragraphs, this information is independently contained in Fig. 4(b). The T_e-profile in the 2DEG strip is given by (see supplementary material[18])
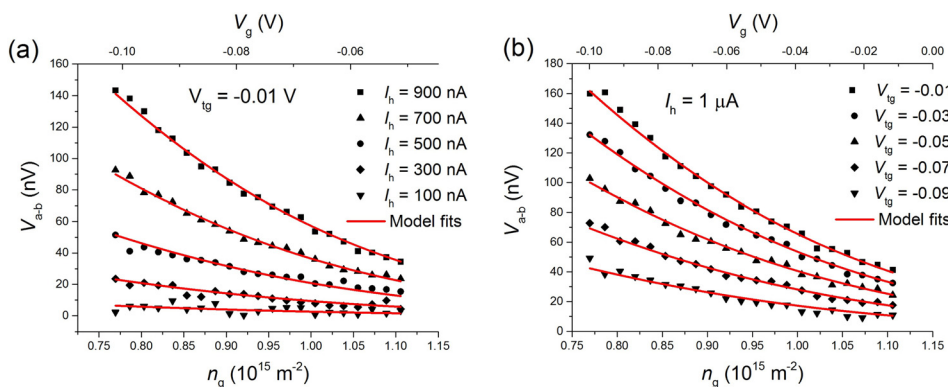

FIG. 3. Fits to the data using Eqs. (2)–(4). The graphs show V_{th} as a function of the swept gate voltage V_g and n_g, the corresponding carrier density under the swept gate. The different traces in (a) and (b) represent different heating currents I_h and different top-gate voltages V_{tg}, respectively. The fits are markedly improved over, for example, that shown in Fig. 2.
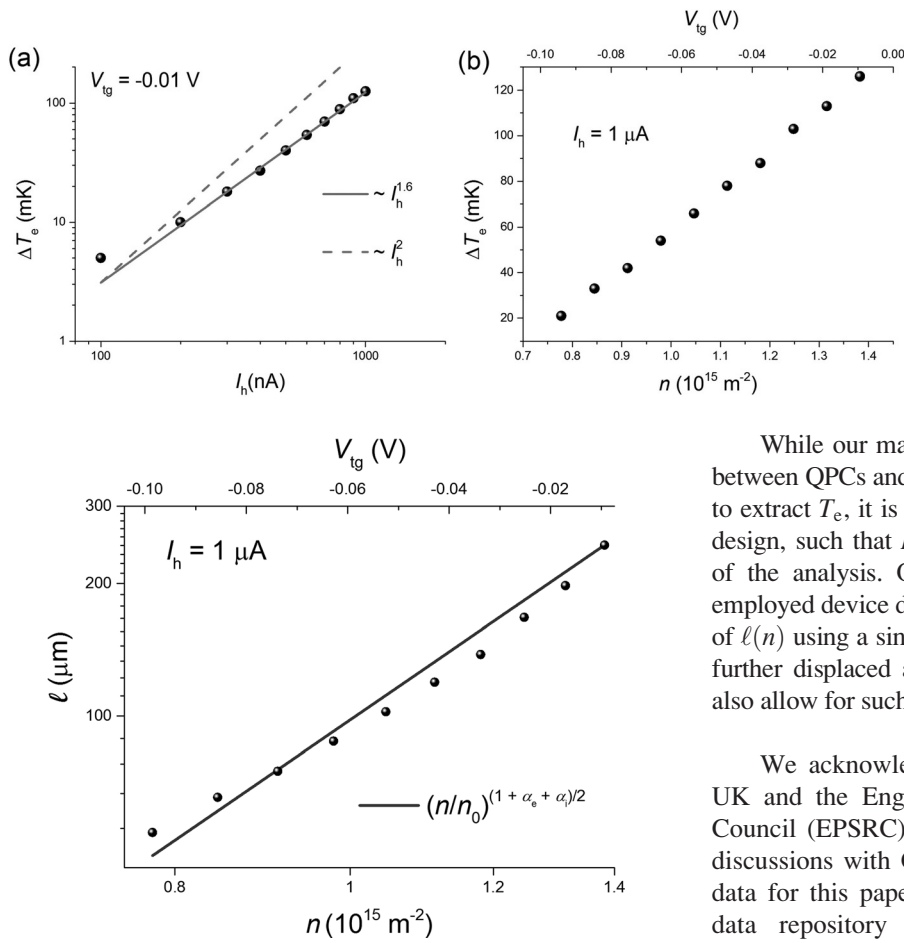
FIG. 4. (a) The elevated electron temperature $\Delta T_e \equiv T_e - T_L$ extracted from the model is seen to increase as a power-law of I_h. The broken line shows a I_h^2 trend, which would be the case if ΔT_e increased linearly as a function of applied heating power. The sub-linear dependence on power indicates that there are heat losses to the surrounding lattice. (b) As V_{tg} becomes more negative, T_e at the first thermometer decreases rapidly, indicating that the electrons thermalize over a much shorter distance.

FIG. 5. Energy relaxation length ℓ as a function of carrier density n. The data in Fig. 4(b) produce an independent measure of $\ell(n)$ which we find to be in excellent agreement with the model exponents.

$$\Delta T_e(y) = \Delta T_{e,0} \frac{\sinh\left[(L_{strip} - y)/\ell\right]}{\sinh\left(L_{strip}/\ell\right)}. \qquad (5)$$

Here, y is the spatial coordinate along the 2DEG strip (see Fig. 1(b)) and $\Delta T_{e,0} \equiv \Delta T_e(y = 0)$, the temperature elevation in the heating channel. Since the heating channel is effectively at a constant temperature between pairs of points in Fig. 4(b), the ratio $\Delta T_e(n_1)/\Delta T_e(n_2)$ taken at $y = L_{T1}$ provides an implicit relation between $\ell(n_1)$ and $\ell(n_2)$, where n_1 and n_2 are the respective carrier densities. Therefore, this allows the inference of ℓ from T_e, and reconstruction of ℓ as a function of n as shown in Fig. 5. This is the main result of this study showing the dependence of the energy relaxation length scale on the carrier density. We stress that this is a *direct* measurement of $\ell(n)$ using the pre-calibrated BGT, which we find to be in striking agreement with indirectly obtained dependence $\ell(n) = \ell_0(n/n_0)^{(1+\alpha_e+\alpha_i)/2}$, using the values of ℓ_0 and α_i derived from the model and the fitting.

To summarize, we have demonstrated that BGTs are a versatile tool with which to detect elevated electron temperatures. As remarked earlier, BGTs are an attractive alternative to QPCs. QPC fabrication requires electron beam lithography and they come with the associated difficulties of sub-micrometre devices such as sensitivity to electrical shock and vulnerability to disorder. In contrast, BGTs can be macroscopic and therefore free from the above mentioned difficulties.
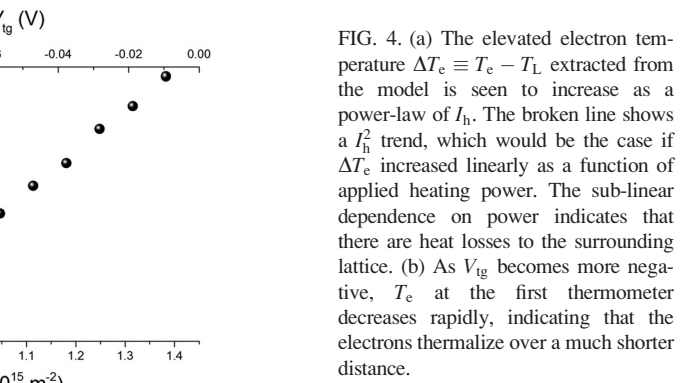
While our manuscript seems to suggest that the trade-off between QPCs and BGTs is that detailed modelling is required to extract T_e, it is important to note that modifying the device design, such that $L_g > \ell$ significantly reduces the complexity of the analysis. On the other hand, the advantages of the employed device design are that it allows for the determination of $\ell(n)$ using a single BGT. We note that using a second BGT further displaced along the length of the 2DEG strip should also allow for such a measurement, so long as $\ell(n) < L_{T2}$.

[1] J. Davies, *The Physics of Low-Dimensional Semiconductors* (Cambridge University Press, 1998).
[2] A. Mittal, R. G. Wheeler, M. W. Keller, D. E. Prober, and R. N. Sacks, Surf. Sci. **361**, 537 (1996).
[3] L. W. Molenkamp, Th. Gravier, H. van Houten, O. J. A. Buijk, M. A. A. Mabesoone, and C. T. Foxon, Phys. Rev. Lett. **68**, 3765 (1992).
[4] R. T. Syme, M. J. Kelly, and M. Pepper, J. Phys.: Condens. Matter **1**, 3375 (1989).
[5] N. J. Appleyard, J. T. Nicholls, M. Y. Simmons, W. R. Tribe, and M. Pepper, Phys. Rev. Lett. **81**, 3491 (1998).
[6] L. W. Molenkamp, H. van Houten, C. W. J. Beenakker, R. Eppenga, and C. T. Foxon, Phys. Rev. Lett. **65**, 1052 (1990).
[7] M. Wiemann, U. Wieser, U. Kunze, D. Reuter, and A. D. Wieck, Appl. Phys. Lett. **97**, 062112 (2010).
[8] N. F. Mott and M. Jones, *The Theory and the Properties of Metals and Alloys* (Courier Dover, New York, 1958).
[9] O. Chiatti, J. T. Nicholls, Y. Y. Proskuryakov, N. Lumpkin, I. Farrer, and D. A. Ritchie, Phys. Rev. Lett. **97**, 056601 (2006).
[10] Y. Proskuryakov, J. Nicholls, D. Hadji-Ristic, A. Kristensen, and C. Sørensen, Phys. Rev. B **75**, 045308 (2007).
[11] W. E. Chickering, J. P. Eisenstein, and J. L. Reno, Phys. Rev. Lett. **103**, 046807 (2009).
[12] V. Narayan, M. Pepper, J. Griffiths, H. Beere, F. Sfigakis, G. Jones, D. A. Ritchie, and A. Ghosh, Phys. Rev. B **86**, 125406 (2012).
[13] V. Narayan, E. Kogan, C. Ford, M. Pepper, M. Kaveh, J. Griffiths, G. Jones, H. Beere, and D. A. Ritchie, J. Low Temp. Phys. **171**, 626 (2013).
[14] V. Narayan, E. Kogan, C. Ford, M. Pepper, M. Kaveh, J. Griffiths, G. Jones, H. Beere, and D. Ritchie, New J. Phys. **16**, 085009 (2014).
[15] S. Rojek and J. König, Phys. Rev. B **90**, 115403 (2014).
[16] M. Baenninger, A. Ghosh, M. Pepper, H. E. Beere, I. Farrer, P. Atkinson, and D. A. Ritchie, Phys. Rev. B **72**, 241311(R) (2005).
[17] A. Ganczarczyk, S. Rojek, A. Quindeau, M. Geller, A. Hucht, C. Notthoff, J. König, A. Lorke, D. Reuter, and A. D. Wieck, Phys. Rev. B **86**, 085309 (2012).
[18] See supplementary material at http://dx.doi.org/10.1063/1.4926338 for supporting text and data.